4 ALTERATIONS TO PNPLA3 IN HEPATOCYTES LEADS TO INCREASED LIPID ACCUMULATION AND ALTERED RESPONSE TO LIPID-INDUCED STRESS

4.1 Introduction

At its core, NAFLD is a disease of disrupted fatty acid homeostasis. When the concentration of incoming fatty acids overwhelms a hepatocyte's ability to properly store or metabolize those fatty acids, steatosis and eventually lipotoxicity result. Fatty acids are biologically active metabolites that have many functions ranging from energy source to signalling molecule [230]. Free fatty acids have several possible fates upon entering a hepatocyte. These fatty acids can be exported to other tissues such as adipose tissue via VLDL secretion, esterified into triglycerides for storage, or metabolized to produce energy through β-oxidation.

The first line of defence a hepatocyte has against increased fatty acid influx is fatty acid efflux. When the lipid concentration in a hepatocyte gets too high, the cell upregulates VLDL secretion in order to re-establish homeostasis. The capacity for fatty acid efflux via VLDL secretion is extremely high, but the process is saturable. It has also been shown that hepatocellular stress such as that caused by NASH reduces the VLDL export capacity by reducing the production of APOB-100 [64]. When the concentration of fatty acids exceeds the export capacity of the hepatocyte, the remaining fatty acids must either be stored or metabolized, each of which has a differential effect on the viability of the cell.

The esterification of free fatty acids into triglycerides is generally viewed as a cytoprotective process. Triglycerides are metabolically inert molecules that can be stored in lipid droplets indefinitely with little or no effect on the health of a hepatocyte. When faced with a large burden of metabolically harmful free fatty acids, hepatocytes shunt these fatty acids into triglyceride storage [35, 231]. If the increased lipid flux continues for a prolonged period of time, steatosis develops. For this reason, there remains significant debate in the research community about whether steatosis is a pathogenic step in NAFLD progression or if it is merely an epiphenomenon that results from hepatocytes' attempt to buffer themselves from increased fatty acid flux [232, 233].

Alternately, free fatty acids that are metabolized by β-oxidation or other metabolic pathways can cause significant damage to the cell. The process of β-oxidation generates ROS. At normal physiological levels, these ROS are neutralized by the antioxidant

defence systems in the cell. However, when faced with pathological levels of free fatty acids, β-oxidation and other metabolic processes are starkly upregulated to address the increased lipid burden. This upregulation of metabolism causes increased ROS production which overwhelms the antioxidant capacity of hepatocytes. The un-neutralized ROS then wreak havoc on the cell by causing lipid peroxidation, ER stress, and mitochondrial dysfunction. If this insult persists and cannot be controlled by cell defence pathways such as the unfolded protein response, the hepatocyte will succumb to lipotoxicity [64, 79, 80]. This lipoapoptosis results in the release of pro-inflammatory and pro-fibrotic mediators that facilitate the progression from simple steatosis to NASH.

The PNPLA3 protein has been hypothesized to play a role in each of the aforementioned aspects of fatty acid homeostasis. It is believed that the pathogenic effects of the I148M variant result from disruption to at least one of these processes. It has been demonstrated previously that patients homozygous for the risk allele have lower circulating levels of lipoproteins and *in vitro* studies have suggested that this phenomenon is a result of reduced VLDL export in these patients [122]. It is possible that in its role as a lipid droplet remodelling protein, PNPLA3 may sequester triglycerides in lipid droplets and thereby prevent their export in VLDL which in turn exacerbates steatosis. PNPLA3 has also been shown to have LPAAT activity and actively participate in the formation of triglycerides. The I148M variant is hypothesized to increase this function thereby causing steatosis through increased generation of triglycerides [118]. However, the veracity of these claims has recently been called into question due to concerns regarding the experimental approach and the inability to confirm these findings *in vivo* [111]. Finally, the most well-established role for PNPLA3 is its lipolysis activity. Lipolysis is one of the first steps in the β-oxidation of triglycerides thus connecting PNPLA3 to each fatty acid disposal pathway within hepatocytes. The I148M variant causes a loss of lipolytic activity which causes increased triglyceride accumulation and steatosis [109, 121, 164]. Each of these proposed functional roles for PNPLA3 result in the sequestration of neutral lipids rather than increased metabolic activity which can result in hepatocellular damage. This sequestration of triglycerides by reduced VLDL export, increased triglyceride formation, or decreased triglyceride lipolysis offers mechanistic insight into how the I148M variant

induces steatosis; however, these mechanisms fail to explain the progressive nature of PNPLA3-induced NAFLD.

Given the biological significance of free fatty acids in the pathogenesis of NAFLD and the role of PNPLA3 in the fate of hepatic free fatty acids, we chose to use palmitic acid and oleic acid in our *in vitro* model of PNPLA3-induced NAFLD. Palmitic acid is a saturated fatty acid (SFA) while oleic acid is a monounsaturated fatty acid (MUFA). SFAs are metabolically destructive lipid species because they are primed for entry to several metabolic pathways that generate ROS including β-oxidation and are used to synthesize other damaging lipid species such as LPC and ceramides [80, 81]. Additionally, when high concentrations of SFAs are incorporated into phospholipid membranes, the fluidity of the membranes is reduced resulting in cell stress and apoptosis. Alternately, MUFAs are almost exclusively incorporated into triglycerides rather than participating in metabolic pathways. Cells treated with high concentrations of MUFAs develop steatosis without suffering any loss of viability [234]. Given their differential roles in lipid metabolism, we chose to use oleic acid and palmitic acid to model two aspects of NAFLD disease progression: steatosis and lipotoxicity, respectively. In order to model NAFLD *in vitro*, we sought to use a physiological concentration of free fatty acids in our system. However, clinical data on the reference ranges of plasma fatty acid concentrations are extremely limited. The concentration of free fatty acids in the serum varies extensively and can be influenced by the feeding/fasting cycle as well as conditions such as obesity and type 2 diabetes. In addition, it is difficult to quantify the concentration of free fatty acids that hepatocytes are directly exposed to as collecting blood samples from the portal vein is quite invasive. A recent profile of plasma fatty acid concentrations in healthy adults found that the concentration of palmitic acid varied from 0.3 to 4.1 mM while the concentration of oleic acid varied from 0.03 to 3.2 mM [235]. Similarly, studies have found that NAFLD patients have elevated plasma levels of both palmitic and oleic acid [236]. Given this clinical data, as well as previous *in vitro* studies using the aforementioned fatty acids, we chose to use a fatty acid concentration of 250 μM for our experiments. In order to facilitate fatty acid uptake by our HLCs, the free fatty acids were first conjugated to BSA at a molar ratio of 1.66:1 FFA to BSA.

In this chapter, we generated an *in vitro* model to better understand the role of PNPLA3 in NAFLD development and progression. First, PNPLA3^{UC}, PNPLA3^{I148M}, and PNPLA3^{KO} cells were differentiated into HLCs and placed in 3D culture. The lines were then treated with either control media or media supplemented with 250 μM oleic acid or 250 μM palmitic acid to induce a steatotic or lipotoxic phenotype, respectively. The cells were treated with the free fatty acids for up to one week and the phenotypic differences between lines were assessed. We began by quantifying the lipid accumulation in each of the lines using immunofluorescence microscopy and flow cytometry. We then assessed the reaction of each genotype to lipid induced stress by measuring viability and expression of ER stress markers. Finally, we examined the question of whether the I148M variant is a loss of function or gain of function variant using transcriptomic analyses.

4.2 PNPLA3 edited cells accumulate more lipids than untargeted control cells

The I148M variant of PNPLA3 has been robustly correlated with increased hepatic lipid accumulation [91, 123, 134]. In order to assess the effect of *PNPLA3* genotype on lipid accumulation in our system, we began by differentiating PNPLA3^{UC}, PNPLA3^{I148M}, and PNPLA3^{KO}, cells into HLCs and placing them in 3D culture. The HLCs were then treated for one week with control media or media supplemented with fatty acids. The media used for these experiments had a high concentration of glucose and its derivatives in order to stimulate de novo lipogenesis and increase lipid accumulation to the fullest extent possible. Following the one week of treatment, lipid accumulation was assessed qualitatively using immunofluorescence microscopy and quantitatively using flow cytometry. We used Bodipy to stain the neutral lipids in the cells and visualize the lipid droplets. We performed each of these experiments on both the FSPS13B and A1ADR/R cell lines.

Based upon the characteristics of the fatty acids, we expected that, in PNPLA3^{UC} cells, the oleic acid would induce profound steatosis while the palmitic acid would result in only a small amount of lipid accumulation due to its cytotoxicity. Based upon the clinical evidence, we hypothesized that PNPLA3^{I148M} cells would accumulate more lipid droplets than PNPLA3^{UC} cells and be more susceptible to lipid-induced stress. Due to the lack of

phenotype seen in mice with a complete knock-out of the Pnpla3 protein, we hypothesized that the PNPLA3^{KO} cells would mimic the PNPLA3^{UC} cells phenotypically.

Figures 4.1 shows representative micrographs of the PNPLA3^{UC}, PNPLA3^{I148M}, and PNPLA3^{KO} lines treated with control medium, oleic acid, or palmitic acid in the FSPS13B background. These images show that PNPLA3^{UC} cells behaved exactly as hypothesized. These cells accumulated a small number of lipid droplets under basal conditions. The oleic acid induced a stark steatotic phenotype with nearly all of the cytoplasmic space being occupied by microstetotic lipid droplets. The palmitic acid treated cells accumulated a very small amount of lipid droplets, much more closely resembling the control treated cells rather than the oleic acid treated cells. As expected, the PNPLA3^{I148M} cells accumulated more lipid droplets in all treatment groups than their PNPLA3^{UC} counterparts. Interestingly, the PNPLA3^{I148M} cells were extremely steatotic when treated with both oleic acid and palmitic acid. Strikingly, contrary to our original hypothesis, the PNPLA3^{KO} cells accumulated the most lipid droplets of all the genotypes regardless of treatment type. The PNPLA3^{KO} line had the highest basal level of lipid accumulation and followed the same phenotypic pattern of response as PNPLA3^{I148M} cells to oleic acid and palmitic acid treatment. Notably, the lipid droplets in PNPLA3^{KO} cells appeared to be qualitatively larger than PNPLA3^{UC} cells. This phenomenon has been noted before in *in vitro* overexpression models of the PNPLA3 I148M variant [109].

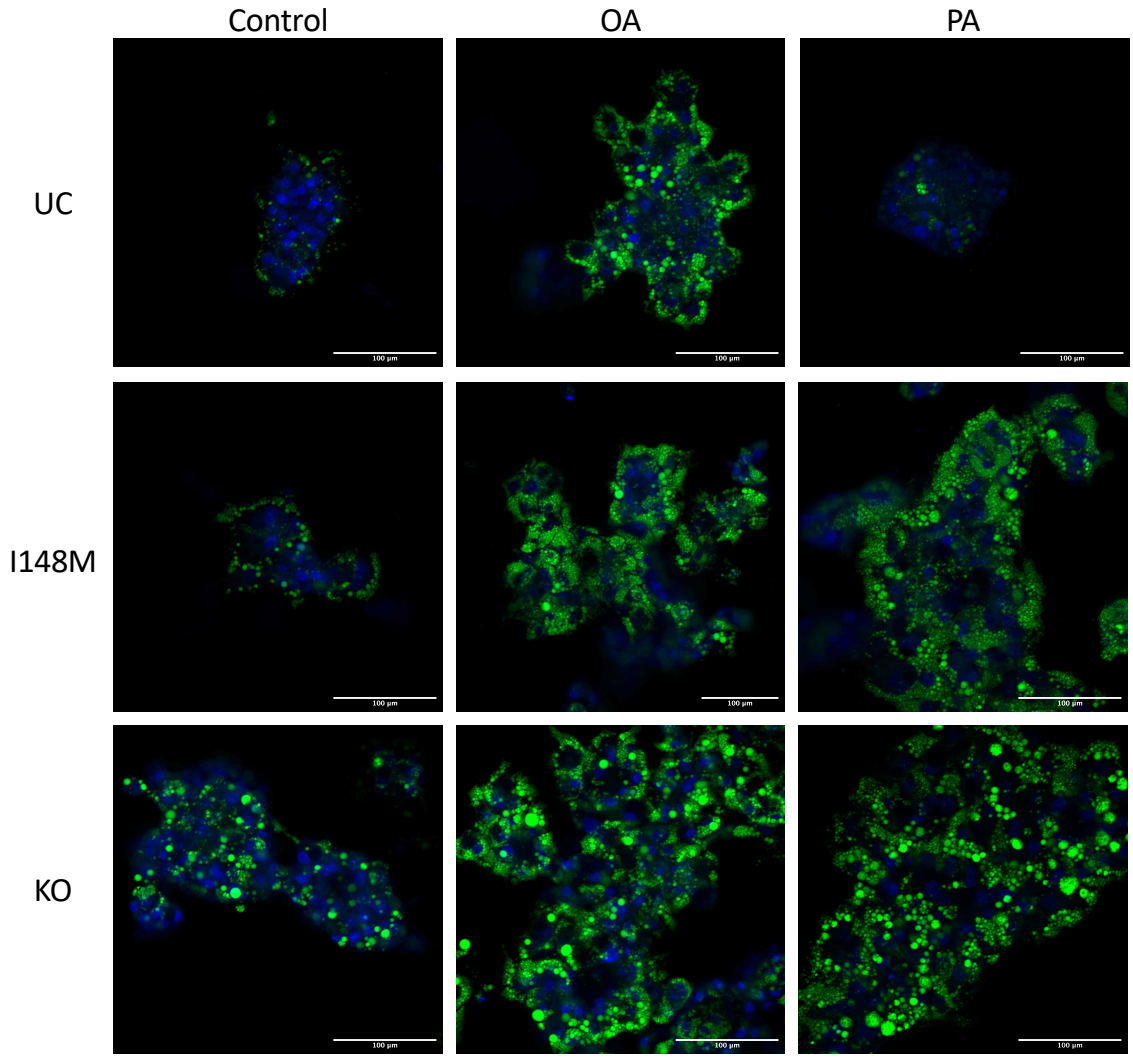

Figure 4.1 Lipid droplet accumulation in FSPS13B lines.

Representative images of bodipy stained lipid droplets in cells from the three genotypes. Regardless of treatment type, progressively more lipids were accumulated in PNPLA3^{I148M} cells and PNPLA3^{KO} cells than PNPLA3^{UC} cells. This experiment was performed 6 times and the best representative images are represented in this figure.

Both the PNPLA3^{I148M} and PNPLA3^{KO} lines accumulated more lipid droplets than PNPLA3^{UC} cells and failed to metabolically differentiate between SFAs and MUFAs when esterifying triglycerides and forming lipid droplets. This failure to differentiate between the metabolic roles of the two classes of fatty acids leads to increased triglyceride storage and steatosis. These results, in stark contrast with the results from murine knock-out experiments, indicate that the loss of PNPLA3 protein causes enhanced steatosis in

human hepatocytes. These data argue that the pathogenic mechanism of the I148M variant is facilitated through a loss of function.

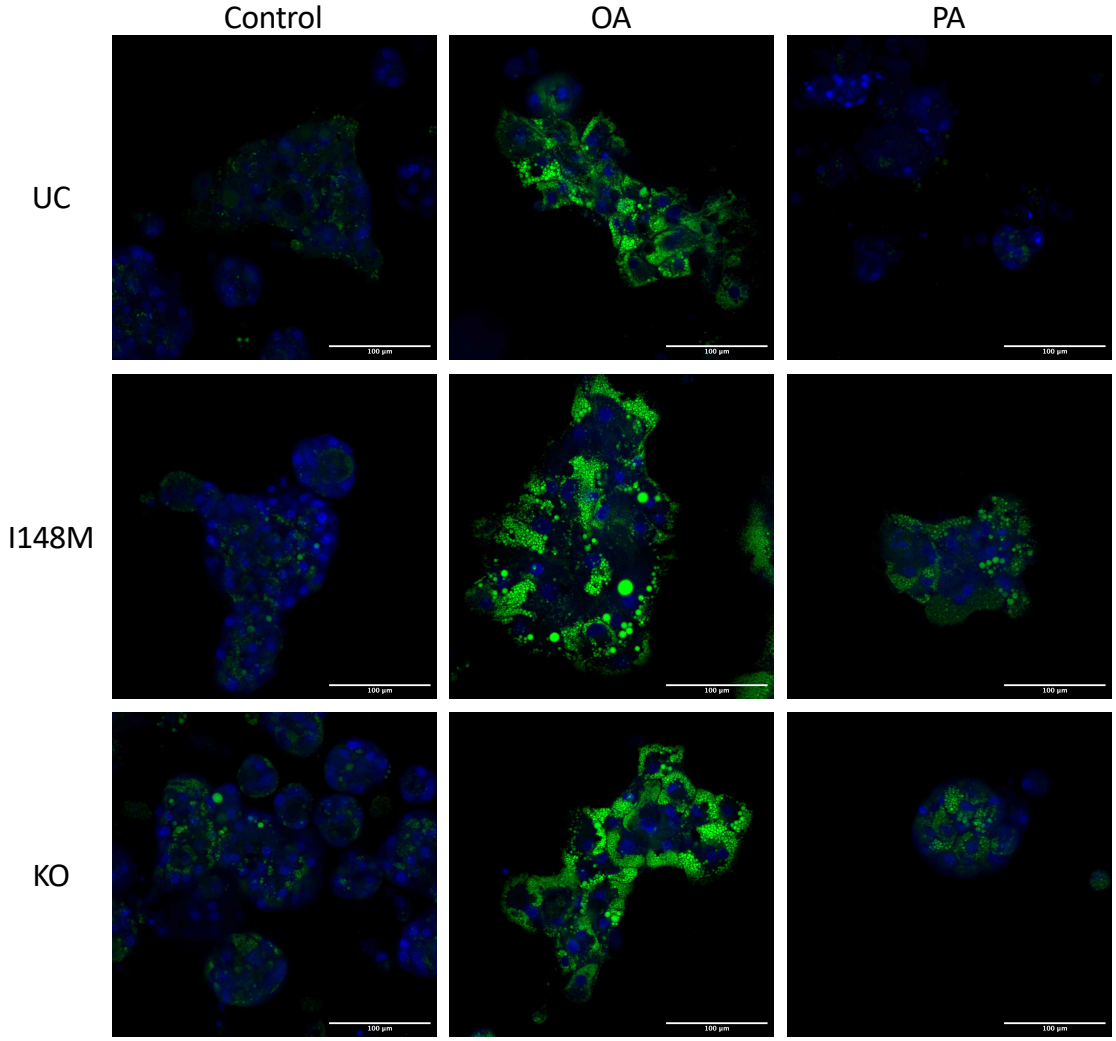

Figure 4.2 Lipid droplet accumulation in A1ATDR/R lines.

Representative images of bodipy stained lipid droplets in cells from the three genotypes. Regardless of treatment type, progressively more lipids were accumulated in PNPLA3^{I148M} cells and PNPLA3^{KO} cells than PNPLA3^{UC} cells. This experiment was performed 1 time and the best representative images are represented in this figure.

In order to confirm these findings, we performed the same experiment in the A1ATDR/R lines (Figure 4.2). At basal levels, the A1ATDR/R lines appeared to accumulate fewer lipid droplets than their FSPS13B counterparts, regardless of genotype. However, the phenotypic pattern of lipid accumulation in this genetic background was consistent with the results from the previous experiment for all three genotypes. The PNPLA3^{UC} cells

had a very low amount of basal lipid accumulation, exhibited a steatotic phenotype when treated with oleic acid, and nearly undetectable levels of lipid accumulation when treated with palmitic acid. Both the PNPLA3^{I148M} and PNPLA3^{KO} lines had higher basal lipid accumulation and steatotic phenotypes when treated with both oleic acid and palmitic acid. In this line, the palmitic acid appears to induce slightly less lipid accumulation than oleic acid indicating that this genetic background may be slightly more proficient at differentiating between the saturation status of different fatty acids in the absence of PNPLA3. Additionally, the PNPLA3^{I148M} cells accumulated significantly larger lipid droplets than the PNPLA3^{UC} and PNPLA3^{KO} lines in this genetic background. Overall, the data from the A1ATDR/R lines confirms the findings in the FSPS13B line. Namely, loss of PNPLA3 function causes steatosis and increased lipid droplet size. This steatosis is facilitated, at least in part, by the failure to differentiate between SFAs and MUFAs when partitioning fatty acids into triglyceride storage.

In order to confirm these qualitative observations, we used flow cytometry to quantify the differences in lipid accumulation between genotypes. Unfortunately, we faced technical difficulties in removing the cells from the 3D matrix and dissociating them while maintaining a high cell viability. Therefore, we chose to perform flow cytometric analyses on cells treated with fatty acids in 2D. These analyses confirmed the microscopy results. As before, the FSPS13B lines had higher basal lipid accumulation than the A1ATDR/R lines. In both the FSPS13B and A1ATDR/R lines, there was a stepwise increase in lipid accumulation from PNPLA3^{UC} cells to PNPLA3^{I148M} cells to PNPLA3^{KO} cells in all three treatment groups (Figure 4.3). This analysis revealed that the PNPLA3^{I148M} cells possess an intermediate phenotype between PNPLA3^{UC} cells and PNPLA3^{KO} cells as would be expected for an incomplete loss of function variant. In the A1ATDR/R lines, the PNPLA3^{I148M} and PNPLA3^{KO} lines accumulated significantly more lipids than the PNPLA3^{UC} cells in all three treatment groups. In the FSPS13B line, PNPLA3^{KO} cells accumulated significantly more lipid droplets that PNPLA3^{UC} lines in all treatment groups while the differences between PNPLA3^{I148M} and PNPLA3^{UC} only reached statistical significance in the PA treatment group. Indicating once again that saturated fatty acids induce the most profound phenotype when PNPLA3 protein function is lost.

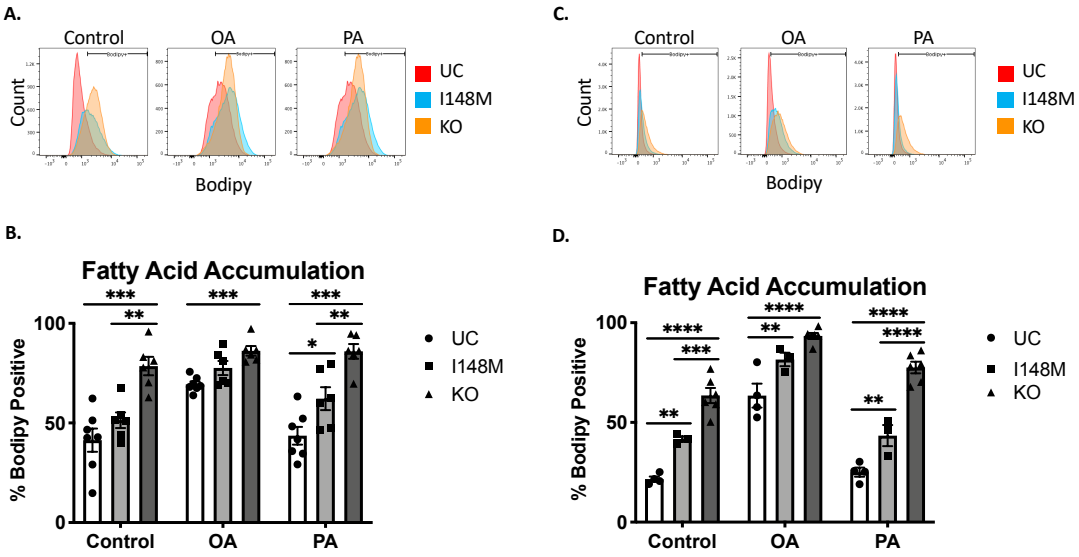

Figure 4.3 Flow cytometric analysis of lipid accumulation.

A. Representative flow cytometric analysis of lipid accumulation via bodipy staining in FSPS13B cell lines. **B.** Quantification of the percentage of bodipy positive cells in A ($PNPLA3^{UC}$: n = 2 clones and 5 independent experiments; $PNPLA3^{I148M}$: n = 2 clones and 5 independent experiments; $PNPLA3^{KO}$: n = 3 clones and 2 independent experiments). There was a stepwise increase in lipid accumulation from $PNPLA3^{UC}$ to $PNPLA3^{I148M}$ to $PNPLA3^{KO}$ cells. **C.** Representative flow cytometric analysis of lipid accumulation via bodipy staining in A1ATDR/R cell lines. **D.** Quantification of the percentage of bodipy positive cells in C ($PNPLA3^{UC}$: n = 2 clones and 4 independent experiments; $PNPLA3^{I148M}$: n = 1 clones and 3 independent experiments; $PNPLA3^{KO}$: n = 2 clones and 4 independent experiments). These results are consistent with the FSPS13B line as well as the disease phenotype. Ordinary one-way ANOVAs with Dunnett's multiple comparisons tests were performed to test statistical significance between means. Error bars represent SEM.

Overall, we found that $PNPLA3^{I148M}$ and $PNPLA3^{KO}$ cells accumulate more, larger lipid droplets than $PNPLA3^{UC}$ cells. The $PNPLA3^{I148M}$ cells appear to have an intermediate phenotype between $PNPLA3^{UC}$ and $PNPLA3^{KO}$ cells indicating that the I148M variant may cause steatosis through a loss of enzymatic function. Additionally, loss of PNPLA3 function results in increased steatosis regardless of treatment type. $PNPLA3^{I148M}$ and $PNPLA3^{KO}$ cells appear to lack the ability to differentiate between SFAs and MUFAs when partitioning fatty acids into triglyceride storage. Given that metabolism of SFAs has profound effects on the health of hepatocytes, this lack of discrimination could have profound effects on the metabolism and viability of these cells.

4.3 PNPLA3^{KO} cells are resistant to palmitic acid-induced lipotoxicity

Given the unexpected steatotic effect of palmitic acid in the PNPLA3^{I148M} and PNPLA3^{KO} cell lines, we wanted to further evaluate how PNPLA3 edited cells may react differently to lipid induced stress. We began by differentiating and treating the cells in the same manner as the previous experiments. Following the one week of lipid treatment, the viability of the cells was assessed using the Presto Blue cell viability assay. Additionally, we examined the expression of ER stress markers after 48 hours of lipid treatment in each genotype. We chose the 48-hour timepoint because at that time, cells had accumulated large amounts of lipid droplets but there was not yet a significant effect on viability (data not shown). Therefore, we assumed this timepoint would be ideal for evaluating the reaction of each genotype to lipid induced stress.

The results of the viability assessment for both the FSPS13B lines and the A1ATDR/R lines are shown in Figure 4.4. The viability of the cells was normalized to the control-treated cells in each of the respective genotypes. In the FSPS13B background, the PNPLA3^{UC} line performed exactly as expected. When treated with oleic acid, there was minimal effect on viability, but palmitic acid treatment induced a stark reduction in cell viability to approximately 20% of control-treated cells. This loss of viability was severely blunted in the PNPLA3^{I148M} and PNPLA3^{KO} lines. In the PNPLA3^{KO} line, palmitic acid treatment caused very little cell death with approximately 80% of cells remaining viable following treatment. Similarly, in the PNPLA3^{I148M} line, approximately 60% of cells remained viable following palmitic acid treatment. This line experienced much more variability in viability between experiments. The susceptibility of PNPLA3^{I148M} lines to palmitic acid-induced lipotoxicity may be dependent on the level of enzymatic activity that is retained in the I148M protein.

These results were confirmed in the A1ATDR/R line. Generally, the A1ATDR/R line was more resistant to palmitic acid-induced lipotoxicity. This is likely due to the genotype of the A1ATDR/R line which is naturally heterozygous for the I148M variant. For this reason, the PNPLA3^{UC} line did see a significant reduction in viability following palmitic acid treatment but this reduction was equivalent to that seen in the PNPLA3^{I148M} cells. In

both PNPLA3^{UC} and PNPLA3^{I148M} lines, the cell viability was reduced to approximately 60% of control-treated cells. The PNPLA3^{KO} line remained resistant to this palmitic acid-induced lipotoxicity. This result calls into question whether the A1ATDR/R line was the appropriate confirmation line to choose for such experiments. Patients that are heterozygous for the PNPLA3 risk allele are at increased risk of developing NAFLD albeit less risk than their homozygous counterparts. Thus, even the presence of one risk allele may alter the metabolic phenotype of hepatocytes. The heterozygous nature of the A1ATDR/R line makes it difficult to determine if phenotypic differences between FS13B and A1ATDR/R are driven by the presence of one risk allele or some other difference in their genetic backgrounds. However, since the I148M variant exerts its pathogenicity in an additive manner, we do believe that some insight may be gained from experiments with the A1ATDR/R lines. In each of the experiments that we performed, the FS13B and A1ATDR/R lines mirrored one another showing similar trends between PNPLA3^{UC}, PNPLA3^{I148M}, and PNPLA3^{KO} HLCs with only minor differences in statistical significance in a few experiments. Therefore, despite the heterozygous genotype of the PNPLA3^{UC} cells in this genetic background, we determined that the A1ATDR/R lines were sufficient to use as a confirmatory cell line for the purposes of this thesis. However, in the future, additional efforts should be undertaken in order to confirm these results in another hiPSC line that is homozygous for the PNPLA3 reference allele.

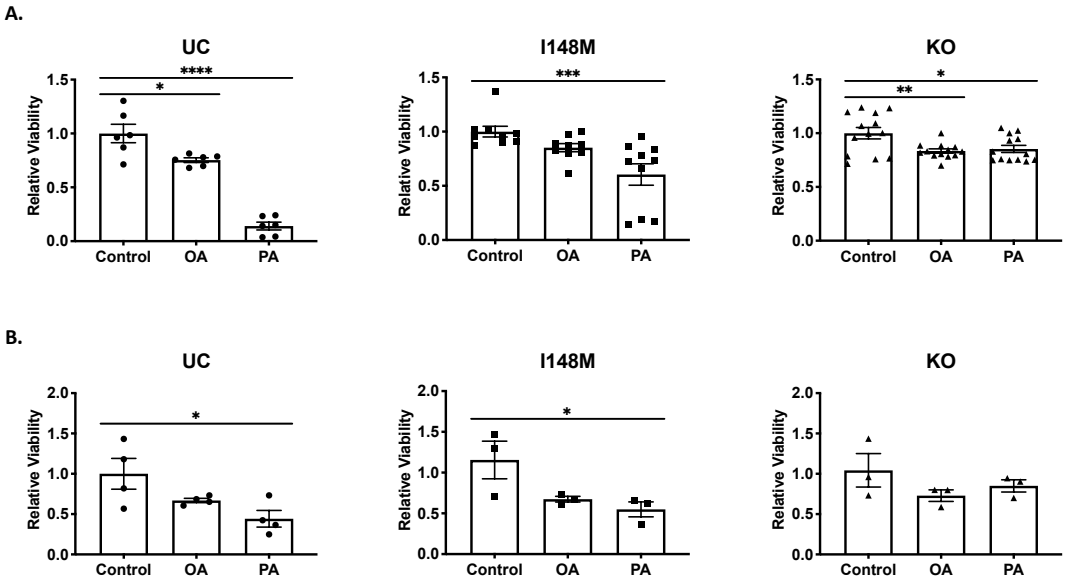

Figure 4.4 Viability of fatty acid treated cells.

Relative viability of FFA treated cells to control cells within each genotype for the **A.** FSPS13B genetic background ($PNPLA3^{UC}$: n = 2 clones and 3 independent experiments; $PNPLA3^{I148M}$: n = 2 clones and 7 independent experiments; $PNPLA3^{KO}$: n = 3 clones and 5 independent experiments) and the **B.** A1ATDR/R genetic background ($PNPLA3^{UC}$: n = 2 clones and 3 independent experiments; $PNPLA3^{I148M}$: n = 1 clones and 4 independent experiments; $PNPLA3^{KO}$: n = 2 clones and 3 independent experiments). $PNPLA3^{UC}$ cells are susceptible to palmitic acid lipotoxicity while $PNPLA3^{KO}$ cells are resistant to the lipotoxic insult of palmitic acid. Ordinary one-way ANOVAs with Dunnett's multiple comparisons tests were performed to test statistical significance between means. Error bars represent SEM.

These data offer an explanation for the increased steatosis observed in $PNPLA3^{I148M}$ and $PNPLA3^{KO}$ lines treated with palmitic acid. In these cell types, palmitic acid appears to be partitioned to triglyceride storage rather than metabolic pathways which results in a decreased lipotoxicity and increased steatosis. Once again, the $PNPLA3^{KO}$ cells demonstrated the most profound phenotype while the $PNPLA3^{I148M}$ cells had an intermediate phenotype between $PNPLA3^{UC}$ and $PNPLA3^{KO}$ cells. There was a similar viability pattern in cells that were heterozygous or homozygous for the I148M variant. This may tentatively indicate that a single risk allele is sufficient to reduce the lipotoxicity of palmitic acid in hepatocytes; however, additional studies are needed to assess this fully.

Previous studies have demonstrated that treatment with palmitic acid leads to an accumulation of di-saturated glycerolipids in the ER membrane [84-86]. The decreased membrane fluidity triggers activation of the unfolded protein response via to IRE1α and PERK pathways. Saturated ER membranes have altered morphology and integrity which disturbs ER proteostasis. The activation of PERK signalling causes the phosphorylation of eIF2α which leads to reduced protein synthesis in an effort to re-establish homeostasis [80]. If the lipotoxic stress persists and the unfolded protein response is unable to re-establish homeostasis, the integrated stress response, regulated by PERK and eIF2α, leads to the transcription of CHOP and GADD34 and the induction of apoptosis [79]. In patients with NAFLD and NASH, PERK expression is starkly upregulated. In addition, the expression of BIP, an ER chaperone protein that plays a role in regulating ER stress, is elevated in patients with NASH. There are conflicting reports regarding the expression level of other downstream activators such as CHOP and GADD34 in these patients [79].

In order to further explore the differential response to lipid-induced stress, we examined markers of ER stress and lipotoxicity. We performed these experiments on the FSPS13B cell lines due to the profound differences between the PNPLA3^{UC} and PNPLA3^{KO} lines. Following 48 hours of lipid treatment, we measured mRNA expression of *BIP, GADD34*, *CHOP*, and *PERK* which are all markers of ER stress and the unfolded protein response (Figure 4.5). In all three genotypes, there was little to no induction of these markers by either control or oleic acid treatment. However, significant differences were observed between genotypes in the palmitic acid treated group. In PNPLA3^{UC} cells, palmitic acid treatment strongly induced all of the cell stress markers, as anticipated. However, the PNPLA3^{I148M} and PNPLA3^{KO} lines largely failed to upregulate these markers. PNPLA3^{KO} cells expressed significantly lower levels of *BIP, GADD34*, and *CHOP* than PNPLA3^{UC} cells while PNPLA3^{I148M} cells expressed significantly lower levels of *BIP, CHOP*, and *PERK*. No significant differences were observed between PNPLA3^{I148M} and PNPLA3^{KO} cells. The failure of these cells to upregulate cell stress markers correlates nicely with the viability data indicating that loss of PNPLA3 function reduces the lipotoxic effects of palmitic acid.

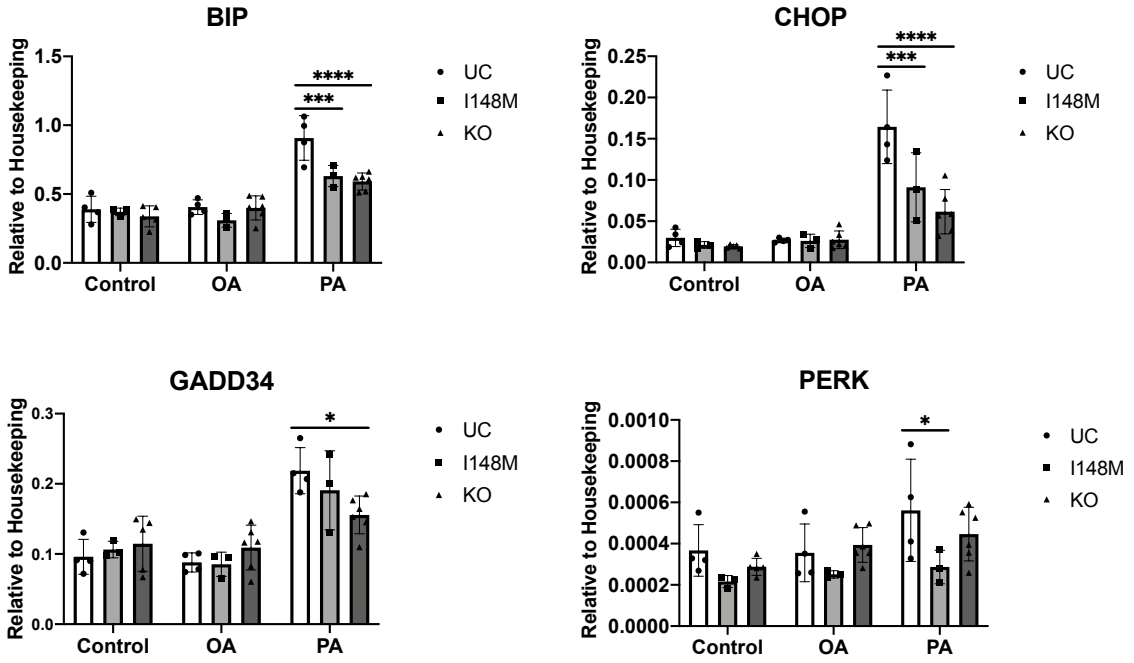

Figure 4.5 Expression of ER stress markers in response to lipid-induced stress.

mRNA expression of ER stress markers *BIP, GADD34, CHOP*, and *PERK* following 48 hours of FFA treatment in cell lines from the FSPS13B genetic background (PNPLA3^{UC}: n = 2 clones and 2 independent

experiments; PNPLA3^{I148M}: n = 2 clones and 2 independent experiments; PNPLA3^{KO}: n = 3 clones and 2 independent experiments). In PNPLA3^{UC} cells, ER stress markers are induced by palmitic acid treatment. PNPLA3^{I148M} and PNPLA3^{KO} cells are resistant to the induction of ER stress markers following palmitic acid treatment. Ordinary one-way ANOVAs with Dunnett's multiple comparisons tests were performed to test statistical significance between means. Error bars represent SEM.

As with the lipid accumulation experiments, analysis of the phenotypic effects of lipid induced stress on these lines revealed stark genotypic differences. We found that the PNPLA3^{UC} lines upregulated ER stress markers and had significantly lower viability when treated with palmitic acid. These results are consistent with lipotoxicity caused by treatment with an abundance of SFAs. Surprisingly, the PNPLA3^{I148M} and PNPLA3^{KO} lines were resistant to this lipotoxicity. These cells largely failed to upregulate markers of cell stress and the palmitic acid treatment did not markedly decreased viability, especially in the PNPLA3^{KO} lines. These results were initially perplexing given the clinical correlation between the I148M variant and severe NASH. We had expected that the cell lines carrying the I148M variant would not only accumulate more lipids, but this increased lipid storage would lead to worsening lipotoxicity that could be used as an *in vitro* surrogate for the severe liver damage seen in NASH patients who carry the I148M variant. However, our results show the opposite trend. We found that loss of PNPLA3 function either through the I148M variant or a complete knock-out of the PNPLA3 protein was cytoprotective against lipid induced stress.

This cytoprotective effect could be a result of several factors. First, these results could indicate that the metabolism of the HLCs is not mature enough to properly model the lipotoxic effects of saturated fatty acids on hepatocytes. However, this seems unlikely given that the PNPLA3^{UC} cells were susceptible to this lipotoxic stressor. Second, it is possible that this cytoprotective effect is a result of off-target effects from the CRISPR/CAS9 editing process. This possibility is equally unlikely given that we used several isogenic lines for each genotype and observed the same trend in two different genetic backgrounds. Third, these results argue that the increased steatosis seen in carriers of the I148M variant may be an epiphenomenon that does not play a role in disease progression. The I148M variant has been clinically correlated to increased inflammation and fibrosis; however, carriers of the risk allele rarely have markers of hepatocellular

damage such as hepatocyte ballooning [132, 151]. Since PNPLA3 is expressed highly in human HSCs and the functionality of these cells is also influenced by the I148M variant, it is possible that the I148M variant has divergent pathological effects on hepatocytes and stellate cells. In hepatocytes, the I148M variant interferes with lipid metabolism causing steatosis which may ultimately be harmless to the cells. In stellate cells, the I148M variant influences the activation state of the HSCs causing increased inflammation and fibrosis which leads to progression from simple steatosis to NASH [113, 114]. Fourth, it is possible that this altered metabolic homeostasis could have detrimental effects on other metabolic pathways of the liver such as drug metabolism. We could hypothesize that the dysregulated metabolism of I148M carriers sensitizes them to other forms of hepatotoxicity. Further investigations are needed to contextualize this seemingly discordant finding in the pathogenesis of human disease.

4.4 The intermediate phenotype of PNPLA3^{I148M} indicates that the variant may be loss of function

The status of the I148M variant as a loss of function or gain of function variant is still a matter of great contention in the scientific community. Several *in vitro* studies claim that the I148M variant causes a loss of enzymatic function, but these results were not corroborated in murine models where Pnpla3 knock-out did not produce any phenotypic changes [109, 118, 122, 160, 161, 165]. We contend that the lack of clarity on this point is due in large part to the lack of an appropriate disease model. The majority of *in vitro* studies were performed on purified enzymes which is a good first step but fails to parse the role of this enzyme in the metabolic activity of the whole cell. Alternately, murine models are not an appropriate model for PNPLA3 pathogenesis due to their low protein homology and extremely low basal expression of Pnpla3 in the liver.

Since our model uses human cells that express an endogenous level of PNPLA3 (data not shown), we believe that this model would be ideal to answer the question of whether the I148M variant in PNPLA3 is a loss of function or gain of function variant. In our initial studies of the PNPLA3^{UC}, PNPLA3^{I148M}, and PNPLA3^{KO} lines, we found that PNPLA3^{I148M} cells had an intermediate phenotype between PNPLA3^{UC} and PNPLA3^{KO} lines. Given these results, we hypothesized that the I148M variant is a loss of function

variant in human hepatocytes. In order to further examine this question, we performed RNA sequencing to examine the transcriptomic differences between the three genotypes. We differentiated the three lines into HLCs, placed them in 3D culture, and treated them with either control, oleic acid, or palmitic acid medium for 24 hours. In order to examine the signalling pathways that influence the phenotypic differences between lines, we chose a time point that allowed ample time for signalling cascades to initiate a cellular response but before any phenotypic differences were observed. The RNA sequencing was performed on the FSPS13B genetic background. At least two lines from each genotype and two differentiations were analysed in order to account for batch effects caused by these variables. Following the sequencing, we performed comparative analyses to examine the transcriptomic differences between PNPLA3^{UC}, PNPLA3^{I148M}, and PNPLA3^{KO} cells when subjected to various lipids.

Figure 4.6a shows the principle component analysis (PCA) plots for the three genotypes treated with control, oleic acid, and palmitic acid medium, respectively. We found that each of the genotypes clustered far away from the others. Genotype was responsible for 60-70% of the variability in the PCA plot. These data indicate that genotype profoundly influences the transcriptome of these cells regardless of treatment. Additionally, each of the genotypes clustered together regardless of cell line and differentiation batch effects. These batch effects were responsible for only 10-20% of the variability in the PCA plot. Thus, the isogenic lines produced robust, reproducible results.

In all three treatment groups, the PNPLA3^{I148M} cells clustered between the PNPLA3^{UC} and PNPLA3^{KO} lines. The PNPLA3^{I148M} lines showed the widest intra-genotype differences, sometimes clustering closer to either PNPLA3^{UC} cells or PNPLA3^{KO} cells. These results are consistent with data from the previous section which showed high intra-genotype variability in the viability of PNPLA3^{I148M} cells when treated with palmitic acid. It appears that different PNPLA3^{I148M} cell lines and/or differentiations cause the cells to behave more like PNPLA3^{UC} or PNPLA3^{KO} lines, respectively. We hypothesize that these differences are caused by different levels of PNPLA3 functionality. This intermediate clustering indicates that the I148M variant is a loss of function variant in human hepatocytes.

In order to further confirm these findings, we compiled heatmaps to visualize the differences in expression pattern between the three genotypes (Figure 4.6b). The heatmap included the top 500 differentially expressed genes between the PNPLA3^{UC} and PNPLA3^{KO} cells for all three treatment groups. Since there were few intra-genotypic differences observed in the PCA plots, we used the average expression of each genotype in the heatmaps for the sake of clarity. These heatmaps clearly demonstrate that the PNPLA3^{UC} and PNPLA3^{KO} lines have divergent expression patterns in all three treatment groups while the PNPLA3^{I148M} cells appear to once again represent an intermediate between the two extremes. These data confirm that in our system, the I148M variant represents a loss of function variant.

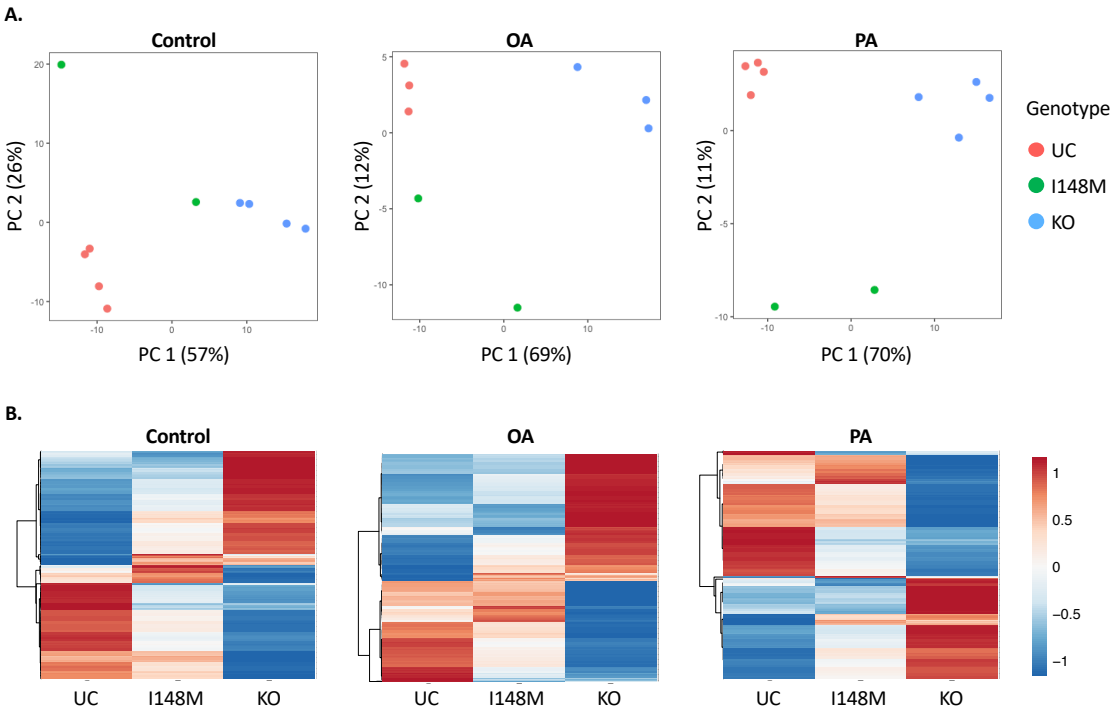

Figure 4.6 Comparative transcriptomic analysis of the three genotypes.

A. PCA plots comparing the three genotypes following the respective treatments (PNPLA3^{UC}: n = 2 clones and 2 independent experiments; PNPLA3^{I148M}: n = 1 clones and 2 independent experiments; PNPLA3^{KO}: n = 2 clones and 2 independent experiments). Regardless of treatment, PNPLA3^{UC} and PNPLA3^{KO} cells clustered far apart from one another while PNPLA3^{I148M} cells are positioned between the two indicating that it represents an intermediate phenotype. **B.** Heatmaps of the top 500 differentially expressed genes between PNPLA3^{UC} and PNPLA3^{KO} cells for each treatment. This once again shows that PNPLA3^{I148M}

cells have a transcriptomic expression profile that is intermediate between those of $PNPLA3^{UC}$ cells and $PNPLA3^{KO}$ cells.

Overall, we found that $PNPLA3^{I148M}$ cells represent a transcriptomic intermediate between $PNPLA3^{UC}$ and $PNPLA3^{KO}$ cells. The $PNPLA3^{I148M}$ cells clustered halfway between the $PNPLA3^{UC}$ and $PNPLA3^{KO}$ cells in principle component analyses of the three genotypes. The transcriptome of these cells varied slightly between differentiations and clustered closer to $PNPLA3^{UC}$ and $PNPLA3^{KO}$ cells, accordingly. We believe that these variations may be a result of fluctuating levels of PNPLA3 functionality between differentiations and cell lines. Additionally, the transcriptomic pattern of the $PNPLA3^{I148M}$ cells was intermediate between the $PNPLA3^{UC}$ and $PNPLA3^{KO}$ cells as visualized by the heatmaps of the top 500 differentially expressed genes. These data robustly confirm the hypothesis that the I148M variant is a loss of function variant in human hepatocytes.

4.5 Conclusions

In this chapter, we used the genetically edited PNPLA3 lines to create an *in vitro* model of NAFLD to investigate the effect of PNPLA3 genotype on lipid accumulation and response to lipid-induced stress. We first differentiated the $PNPLA3^{UC}$, $PNPLA3^{I148M}$, and $PNPLA3^{KO}$ lines into HLCs, placed them in 3D culture, and treated them with control medium or medium supplemented with oleic acid or palmitic acid to induce a steatotic or lipotoxic phenotype, respectively.

Our analyses indicate that $PNPLA3^{I148M}$ and $PNPLA3^{KO}$ lines accumulate more lipid droplets than $PNPLA3^{UC}$ cells in all treatment groups. This phenotype was especially stark in the palmitic acid treated cells. Given this increased lipid accumulation in PNPLA3 edited cells subjected to palmitic acid treatment, we next investigated several phenotypic markers of cell stress. We found that while $PNPLA3^{UC}$ HLCs upregulated the expression of ER stress markers and demonstrated a profound loss of viability when treated with palmitic acid, the $PNPLA3^{I148M}$ and $PNPLA3^{KO}$ HLCs failed to mount such a response to the lipotoxic stimuli. Thus, contrary to the expected result, loss of PNPLA3 function appears to be cytoprotective. In our system, it appears that PNPLA3 edited cells

fail to properly distinguish between SFAs and MUFAs. The PNPLA3 edited cells seem to preferentially shunt SFAs into triglyceride storage rather than other metabolic pathways. This has the dual effect of increasing steatosis in these cells while simultaneously protecting them from the cytotoxic effects of SFAs. Additional studies are needed to contextualize this finding in the pathogenic role of the I148M variant in human disease.

The initial phenotypic data from our model indicated that the I148M variant was most likely a loss of function variant given that the PNPLA3^{I148M} cells trended with the PNPLA3^{KO} cells in all analyses. In order to confirm this, we performed RNA sequencing. We found that the PNPLA3^{I148M} were transcriptomically intermediate between the PNPLA3^{UC} and PNPLA3^{KO} lines. These data confirmed that the I148M variant represents a loss of function variant in our model. The loss of PNPLA3 functionality either through the I148M variant or the complete knock-out profoundly affects the lipid metabolism of the HLCs causing steatosis and an altered response the lipid-induced stress. Though it has been hypothesized for over a decade, based upon clinical and *in vitro* data, our study offers conclusive evidence that the I148M variant is a loss of function variant in human hepatocytes. This *in vitro*, human hepatic system expresses PNPLA3 at an endogenous level, making it potentially invaluable for future studies into the pathogenesis of PNPLA3-induced NAFLD.